Open access • Journal Article • DOI:10.1063/1.4919725

Modeling interface-controlled phase transformation kinetics in thin films

Edward L. Pang, Nhon Q. Vo, T. Philippe, Peter W. Voorhees

Institutions: Northwestern University

Published on: 04 May 2015 - Journal of Applied Physics (AIP Publishing)

Topics: Nucleation, Avrami equation and Phase (matter)

Modeling interface-controlled phase transformation kinetics in thin films

E. Pang, N. Vo, Thomas Philippe, P. Voorhees

AIP Journal of Applied Physics

Modeling interface-controlled phase transformation kinetics in thin films

E. L. Pang, N. Q. Vo, T. Philippe, and P. W. Voorhees

Citation: Journal of Applied Physics **117**, 175304 (2015); doi: 10.1063/1.4919725
View online: http://dx.doi.org/10.1063/1.4919725
View Table of Contents: http://scitation.aip.org/content/aip/journal/jap/117/17?ver=pdfcov
Published by the AIP Publishing

Modeling interface-controlled phase transformation kinetics in thin films

E. L. Pang,[1] N. Q. Vo,[1,2] T. Philippe,[3] and P. W. Voorhees[1]
[1]*Department of Materials Science and Engineering, Northwestern University, Evanston, Illinois 60208, USA*
[2]*NanoAl LLC, Skokie, Illinois 60077, USA*
[3]*Groupe de Physique des Matériaux, Normandie Université, Saint Etienne du Rouvray 76801, France*

(Received 20 February 2015; accepted 22 April 2015; published online 4 May 2015)

The Johnson-Mehl-Avrami-Kolmogorov (JMAK) equation is widely used to describe phase transformation kinetics. This description, however, is not valid in finite size domains, in particular, thin films. A new computational model incorporating the level-set method is employed to study phase evolution in thin film systems. For both homogeneous (bulk) and heterogeneous (surface) nucleation, nucleation density and film thickness were systematically adjusted to study finite-thickness effects on the Avrami exponent during the transformation process. Only site-saturated nucleation with isotropic interface-kinetics controlled growth is considered in this paper. We show that the observed Avrami exponent is not constant throughout the phase transformation process in thin films with a value that is not consistent with the dimensionality of the transformation. Finite-thickness effects are shown to result in reduced time-dependent Avrami exponents when bulk nucleation is present, but not necessarily when surface nucleation is present. © *2015 AIP Publishing LLC*. [http://dx.doi.org/10.1063/1.4919725]

I. INTRODUCTION

The Johnson-Mehl-Avrami-Kolmogorov (JMAK) equation has traditionally been used to study phase transformation kinetics in bulk and thin films. Many researchers, however, have experimentally observed anomalous Avrami exponents and nonlinear Avrami plots in these finite-thickness systems without rigorous explanation.[1–6] The underlying causes for the unusual exponents are explored in this paper.

The JMAK equation is the classical model used to study phase transformation kinetics. While elegant and simple in capturing the kinetic behavior of phase transformations, this model relies on a number of important assumptions:[7–9]

(i) infinitely large system in comparison to the size of individual growing particles
(ii) random homogeneous (bulk) nucleation throughout the entire material
(iii) growth of particles terminates at points of mutual contact but continues unaffected elsewhere.

The above assumptions lead to the key differential relation between volume fraction transformed, f_V, and extended volume fraction, f_V^{ext} (Ref. 8)

$$df_V = (1 - f_V)df_V^{ext}, \tag{1}$$

f_V^{ext} is an artificial fraction taken to be the volume of all growing particles in the system, ignoring impingement, divided by the system volume. Equation (1) states that for any small increase, df_V^{ext}, only a fraction of df_V^{ext} equal to $1 - f_V$ will grow into untransformed material and contribute to df_V. The remainder will overlap with existing transformed material and is subtracted out to account for impingement. Integrating Eq. (1) results in most general form of the JMAK equation[7–11]

$$f_V = 1 - \exp(-f_V^{ext}). \tag{2}$$

When the nucleus size is assumed to be negligible in the isotropic growth regime, the expression for extended volume fraction becomes[12]

$$f_V^{ext} = kt^n, \tag{3}$$

where k is an effective rate constant, and n is the Avrami exponent. Combination of Eqs. (2) and (3) lead to the most widely used form of the JMAK equation

$$f_V = 1 - \exp(-kt^n). \tag{4}$$

Rearranging Eq. (4) yields

$$\ln(-\ln(1 - f_V)) = \ln(k) + n\ln(t). \tag{5}$$

This form elucidates the relationship between $\ln(-\ln(1 - f_V))$ and $\ln(t)$, which are commonly plotted against each other in what is termed an Avrami plot. When the assumptions of the JMAK equation are met, this plot is linear with a slope equal to the Avrami exponent.

For interface-kinetics controlled growth, commonly observed in processes such as recrystallization of deformed grains and polymorphic crystallization, the Avrami exponent traditionally is an integer constant that represents the number of growth dimensions: $n = 1$ corresponds to one-dimensional growth, $n = 2$ corresponds to two-dimensional (2D) growth, and $n = 3$ corresponds to three-dimensional (3D) growth. A constant nucleation rate is also treated as a growth dimension, and n is increased by one in the presence of a constant nucleation rate, i.e., $n = 4$ corresponds to three-dimensional growth with a constant nucleation rate.[12]

In thin films, the assumptions of the JMAK equations are not upheld. As growing particles impinge upon free surfaces, the infinite size assumption is violated. In addition, heterogeneous nucleation from an interface is favored in many systems, violating the random homogeneous (bulk)

nucleation assumption. In each of these cases, Eq. (4) is invalid, and an alternative model is needed.

Limitations of the JMAK equation are widely acknowledged in the literature, and various analytical and computational solutions have been proposed.[13–24] It is generally agreed that a finite system results in a reduced Avrami exponent. Others also suggest that the observed Avrami exponent is not constant as a result. Models accounting for inhomogeneously nucleated systems have also been developed, suggesting that inhomogeneous nucleation results in a reduced Avrami exponent.[13,16,17,23,25–27]

Despite these efforts, no simple model has yet been widely accepted over the existing JMAK equation in such cases, and little work has been done on systematically understanding the evolution of the non-constant Avrami exponents observed in thin film systems. Furthermore, the models proposed in the literature employ complex computations and do not easily lend themselves to data analysis and parameter tuning. Therefore, we propose a computational approach employing the level-set method to investigate the evolution of the Avrami exponent when assumptions of the JMAK equation are not met.

We apply this approach and adjust the nucleation density and film thickness to study their effects on the Avrami exponent and its evolution during the transformation process for the limiting cases of site-saturated bulk and surface nucleation. Results from the simulations can reveal the origins of anomalous Avrami exponents and nonlinear Avrami plots obtained experimentally in thin films.

II. METHODS

The level-set method is a numerical tool commonly used for tracking the evolution of shapes and interfaces over time.[28,29] This method provides a simple description of complicated topology changes, such as when growing particles collide, making it ideal for tracking phase transformations in thin films. Furthermore, since the level-set method is a geometric approach, it is free of any assumptions made by the JMAK equation or other analytical models.

An implicit interface representation was used in this study, which assigns a level-set function $\phi(\vec{x})$ to each particle as a function of position $\vec{x}$. ϕ possesses one extra dimension than the interface being modeled and represents the interface as the $\phi = 0$ isocontour. The choice of ϕ to represent the interface is a signed distance function, which has the desired characteristics of being negative inside the transformed region, positive outside the transformed region, and zero at the interface while maintaining $|\nabla\phi| = 1$.

For isotropic interface-kinetics controlled growth, the particle radius evolves over time as follows:

$$r(t) = r_0 + gt \tag{6}$$

where r_0 is the initial particle radius and g is the interface growth velocity in the normal direction. An r_0 value of 0, corresponding to negligible nucleus size as assumed in Eq. (3), was used for all simulations in this paper. ϕ is then evaluated over time using the following equation of motion:

$$\frac{\partial\phi}{\partial t} + g|\nabla\phi| = 0. \tag{7}$$

To solve the level-set function, the entire three-dimensional Cartesian space is discretized into a mesh of finite size. The mesh spacing was selected to be small enough relative to g to ensure good temporal resolution. The evolving level-set function is then evaluated over the entire domain at each time step using an explicit Euler scheme. The isocontours of ϕ remain spherical (3D simulations) or circular (2D simulations) throughout the entire simulation since they initialized at $t = 0$ in that shape and evolve with constant g. The transformed volume fraction at each time step is computed as the fraction of grid points where $\phi < 0$.

The local Avrami exponent, n, is computed numerically using a five-point stencil according to the following equation proposed by Calka and Radlinski, which can be derived from Eq. (5):[30]

$$n = \frac{d\ln[-\ln(1 - f_V)]}{d\ln(t)}. \tag{8}$$

3D and 2D simulations of phase transformations characterized by site-saturated nucleation were examined to validate our model. Both scenarios reasonably satisfy all assumptions of the JMAK equation. Periodic boundary conditions were imposed in all dimensions to simulate infinite size. Figures 1(a) and 1(b) illustrate 3D and 2D phase transformation processes, respectively, modeled by the level-set method. Figures 2(a) and 2(b) plot the Avrami exponent versus volume fraction transformed for the 3D and 2D phase transformation processes, respectively, modeled by the level-set method. The Avrami exponents obtained were approximately constant and equal to three and two, respectively, as predicted by the JMAK theory. A sharp increase in n is observed at high f_V as the assumptions of the JMAK equation begin to break down. Particles become large relative to the size of the simulation box, and the final growth stages do not obey random impingement as assumed in Eq. (1). This effect becomes less prominent as more particles are placed in the simulation box, in agreement with the findings of Levine *et al.* and Todinov, who derived new analytical expressions in lieu of Eq. (3).[14,15]

III. RESULTS AND DISCUSSION

A. Scaling

To simplify the analysis, we scale all quantities having the dimensions of length by a characteristic length of the system, in agreement with the literature.[16,18] The characteristic length λ is related to the average final particle size after transformation and can be computed from the volume nucleation density, N_V, or area nucleation density, N_A, for the bulk nucleation and surface nucleation cases, respectively, as follows:

$$\lambda = {N_V}^{-1/3}, \tag{9a}$$

$$\lambda = {N_A}^{-1/2}. \tag{9b}$$

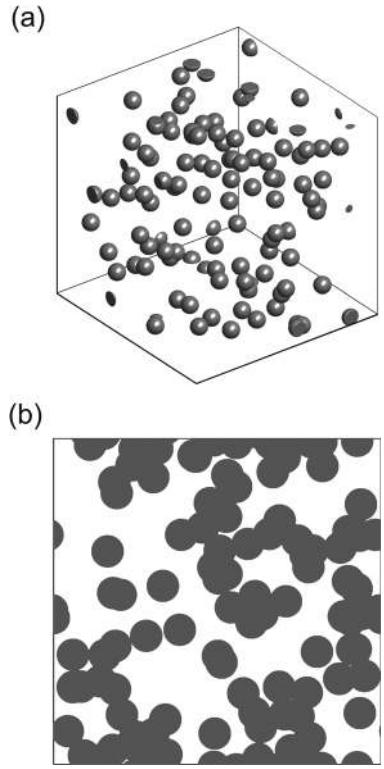

FIG. 1. Visualization of a phase transformation process modeled by the level-set method. These snapshots demonstrate the ability of the level-set method to follow the evolution of complex interfacial morphologies and particle coalescence. (a) 3D simulation of box size 500 × 500 × 500. (b) 2D simulation of box size 1500 × 1500.

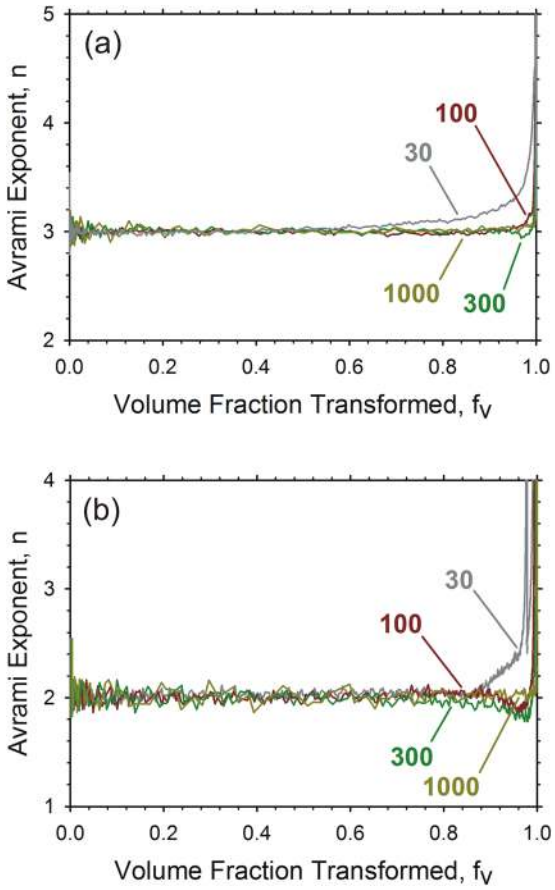

FIG. 2. Avrami exponent vs. volume fraction transformed for site-saturated bulk nucleation reasonably satisfying the assumptions of the JMAK equation. Labels represent the number of particles in the system. Average values over 10 runs with different random initial configurations are displayed. Corresponding visualizations are shown in Figure 1. (a) 3D simulation of box size 500 × 500 × 500. (b) 2D simulation of box size 1500 × 1500.

These definitions are similar to those defined by Trofimov *et al.*[16] However, since the final particle shapes are complicated non-spherical geometries, we drop the spherical shape factor for simplicity.

The effects of nucleation density are related to the absolute film thickness, h, so we encompass both of these parameters in the dimensionless film thickness, h^*, of the system, defined as follows:[16]

$$h^* = \frac{h}{\lambda}. \tag{10}$$

Sections III B–III D discuss our findings on the evolution of the Avrami exponent throughout the phase transformation process in thin films for the bulk and surface site-saturated nucleation cases as a function of h^*.

B. Bulk nucleation

Simulations were conducted using a 1500 × 1500 × 50 box size, with nuclei placed randomly throughout the entire simulation box. Periodic boundary conditions were imposed in the two large dimensions but not the film thickness dimension. To simulate transformations in systems with varying h^* values, the number of nuclei was adjusted in the range between 10 and 900 000. The results are plotted in Figure 3.

For all values of h^*, the initial value of the Avrami exponent is three as the particles grow unconstrained in three dimensions. As particles impinge upon the surfaces of the thin film, n begins to decrease toward two, suggesting a transition from 3D to 2D growth. n approaches two more slowly (in f_V space) as h^* increases (thicker film and/or greater nucleation density) since fewer particles interact with the surfaces (see Figure 4 for a visualization), leading to a growth situation that approaches the bulk 3D limit (see Figure 1(a) for a visualization). For large values of h^*, n approaches a constant value of three, as predicted by the JMAK equation. These results support the general consensus that finite-size effects lead to reduced Avrami exponents.

A few interesting phenomena are observed at the beginning and final stages of transformation (low and high f_V in Figure 3). The noise observed in the first few time steps in all plots is a result of the small particle sizes relative to the mesh size. This issue can be remedied by using a finer mesh, but this significantly increases computation time. The noise observed at high f_V is an artifact of averaging over a set of runs that begin increasing to infinity at different f_V, depending on the random spatial distribution of the nuclei. This effect is diminished with increasing number of particles in the simulation box.

Ocenasek *et al.*[18] studied the effect of film thickness on the Avrami exponent in the presence of a constant nucleation rate by numerically solving an integral expression derived by the authors. Our findings slightly underestimate

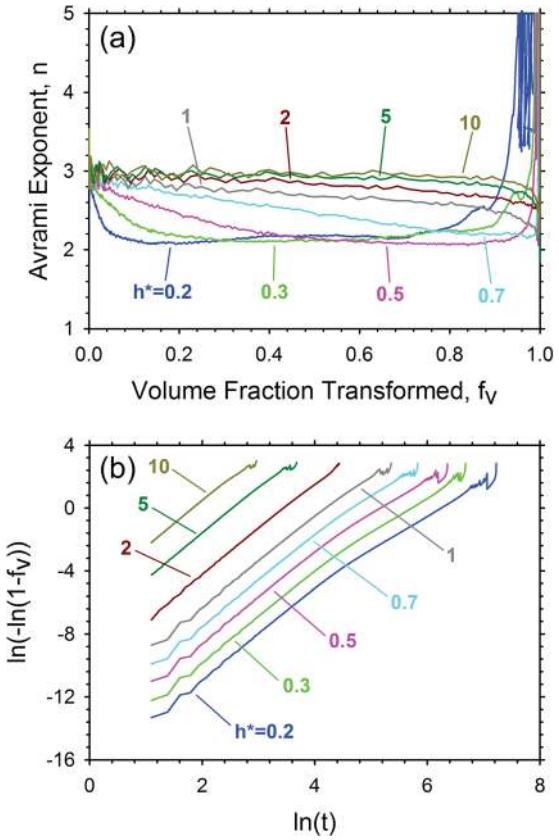

FIG. 3. Evolution of the Avrami exponent as a function of h^* for the bulk nucleation case. Average values over 10 runs with different random initial configurations are displayed. (a) Avrami exponent vs. volume fraction transformed. (b) Avrami plot.

their guidelines, which suggest essentially 2D kinetics for $h^* < 0.3$ and 3D kinetics for $h^* > 10$. For $h^* = 0.3$, we find that the Avrami exponent becomes nearly time independent at a value near two at $f_V \approx 0.3$, but for $h^* = 0.2$, we find that the Avrami exponent becomes nearly time independent at a value near two at $f_V \approx 0.1$ (see plot in Figure 3(a)). We also find little difference between $h^* = 5$ and $h^* = 10$, and the Avrami exponent approximately equals three in both cases. Therefore, we suggest a slightly altered guideline of $h^* < 0.2$ for 2D kinetics and $h^* > 5$ for 3D kinetics. The slight disagreement may be a result of the different definition of characteristic length used by us in comparison to Ocenasek *et al.*

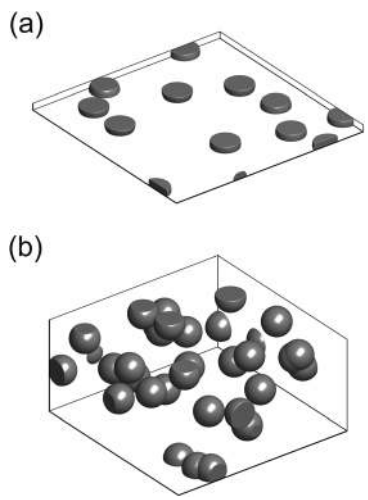

FIG. 4. Visualizations of the phase transformation process for various h^*. Bulk nucleation case. (a) $h^* = 0.2$ (full view, 1500 × 1500×50). (b) $h^* = 2$ (section view, 100 × 100 × 50).

C. Surface nucleation

Simulations were also conducted for the surface nucleation case, again using a 1500 × 1500 × 50 box size with periodic boundary conditions in the two large dimensions only. Two cases were considered: nucleation from one surface only and nucleation from two (both) surfaces. Nuclei were placed randomly on the surface(s). To simulate transformations in systems with varying h^* values, the number of nuclei was adjusted in the range between 100 and 48 000. The results are plotted in Figure 5.

As for the bulk nucleation case, n equals three initially as the particles grow unconstrained in three dimensions. In contrast to the bulk nucleation case, however, n does not immediately decrease since it takes time for the particles growing from the surface(s) to impinge upon the opposite surface. For low h^*, an increase in n is observed initially (see Figures 5(a) and 5(b)). This can be explained as a violation of the uniform random nucleation assumption of the JMAK equation since nuclei are placed only on the surface(s). Because nuclei are sparsely distributed over the surface(s) instead of throughout the entire material, less impingement occurs than assumed in Eq. (1). Therefore, f_V grows more quickly than predicted by the JMAK equation with constant n, and the value of n calculated from Eq. (8) is inflated. This effect is more pronounced for nucleation from one surface than from two surfaces.

The phase transformation kinetics and mechanisms greatly differ depending on the value of h^*. For low values of h^*, most particles reach the surface before interacting with one another (see Figure 6(a) for visualization). When the growing particles impinge upon the opposite surface, a sharp change in behavior occurs as growth transitions from a 3D situation to a 2D situation, and n approaches two, similar to the bulk nucleation case. For high h^*, however, many of the growing particles interact with each other before they impinge upon the surface. The growing particles essentially form a planar front that advances through the thin film, as suggested by Weinberg,[25] which is a 1D growth situation (see Figures 6(b) and 6(c) for visualizations), and n approaches the 1D curve. For intermediate values of h^*, hybrid behavior is observed. The system first transitions from 3D to 1D kinetics. Once the advancing front, which is not perfectly planar, impinges upon the opposite surface, n tends toward a value of two.

The Avrami exponent expression for the 1D planar front case was derived analytically and verified using our level-set simulations and is shown to have the following dependence on volume fraction (plotted with simulation results in Figures 5(a) and 5(b) for comparison):

$$n = -\frac{f_V}{(1-f_V)\ln(1-f_V)}. \tag{11}$$

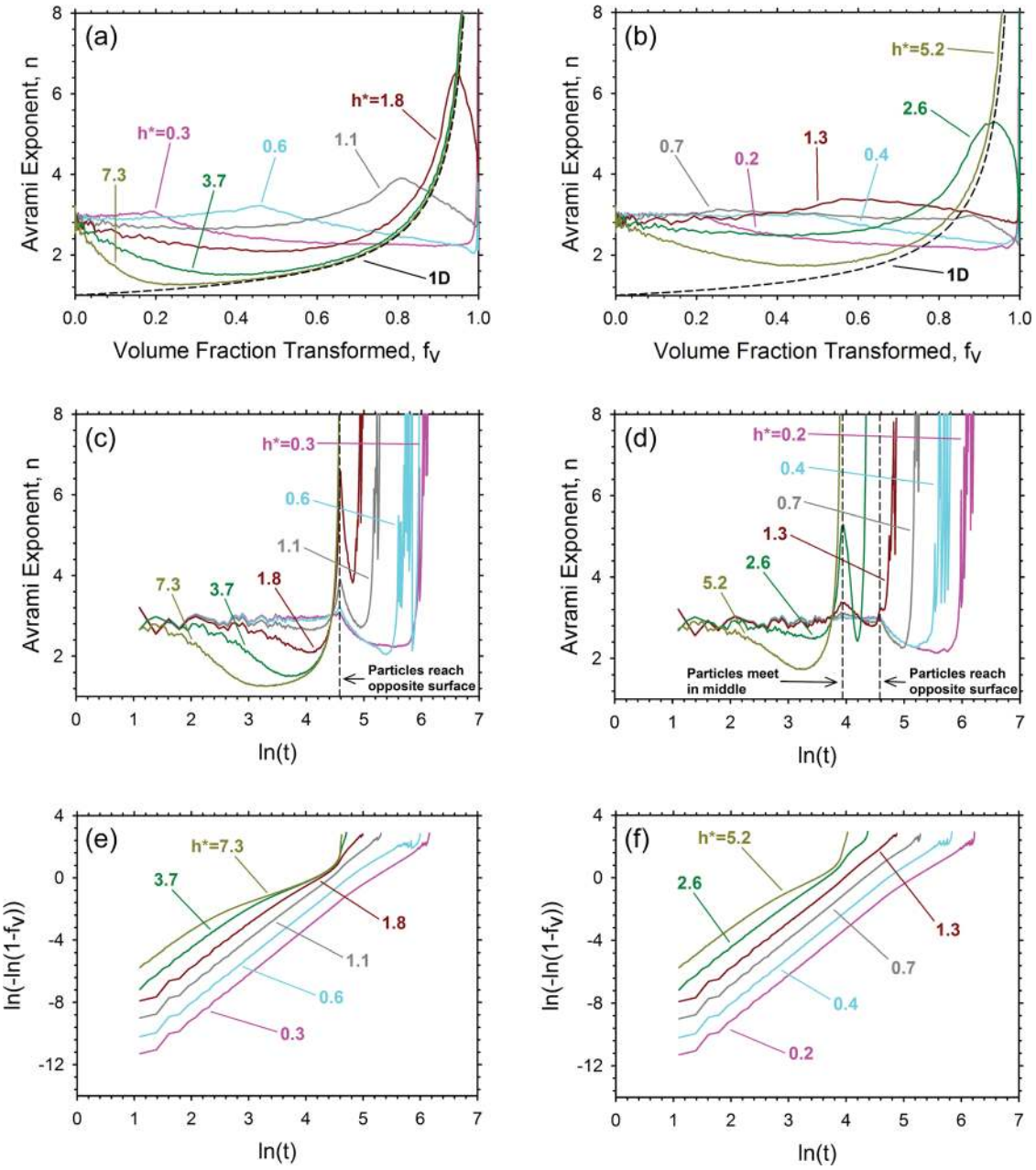

FIG. 5. Evolution of the Avrami exponent as a function of h^* for the surface nucleation case. Average values over 10 runs with different random initial configurations are displayed. (a) Avrami exponent vs. volume fraction transformed (one-surface case). Dashed line represents solution for a 1D planar front, Eq. (11). (b) Avrami exponent vs. volume fraction transformed (two-surface case). Dashed line represents solution for a 1D planar front, Eq. (11). (c) Avrami exponent vs. natural log of time (one-surface case). (d) Avrami exponent vs. natural log of time (two-surface case). (e) Avrami plot (one-surface case). (f) Avrami plot (two-surface case).

The one- and two-surface nucleation cases show similar behavior, but two distinct differences are observed. In the two-surface case, one additional change in behavior occurs when the growing particles from the two opposite surfaces meet in the middle of the thin film. 2D/3D geometries form (see Figure 6(c) for visualization) depending on h^*, and n approaches a value between two and three. This transition is more prominent at high h^* (see Figure 5(d)). Once the growing particles reach the opposite surface, n approaches two as in the one-surface case. This transition is more prominent for low h^* (see plot in Figure 5(d)). This transition does not occur at all for very high h^* since the material is completely transformed when the two advancing fronts meet in the middle of the film. The second distinction is that growth for the two-surface case possesses less 1D character at a given f_V. The two-surface case has a less planar surface than the one-surface case at a given f_V since the two-surface case has less distance for the advancing front to flatten out (see Figures 6(b) and 6(c) for visualizations).

In many cases, we observed an increase in n at some stage during the transformation process as a result of inhomogeneous surface nucleation. Sun *et al.* previously found that, by solving an integral expression derived by the authors, inhomogeneous nucleation results in reduced Avrami exponents.[27] The authors, however, studied this phenomenon in much thicker systems ($215 < h^* < 1598$)

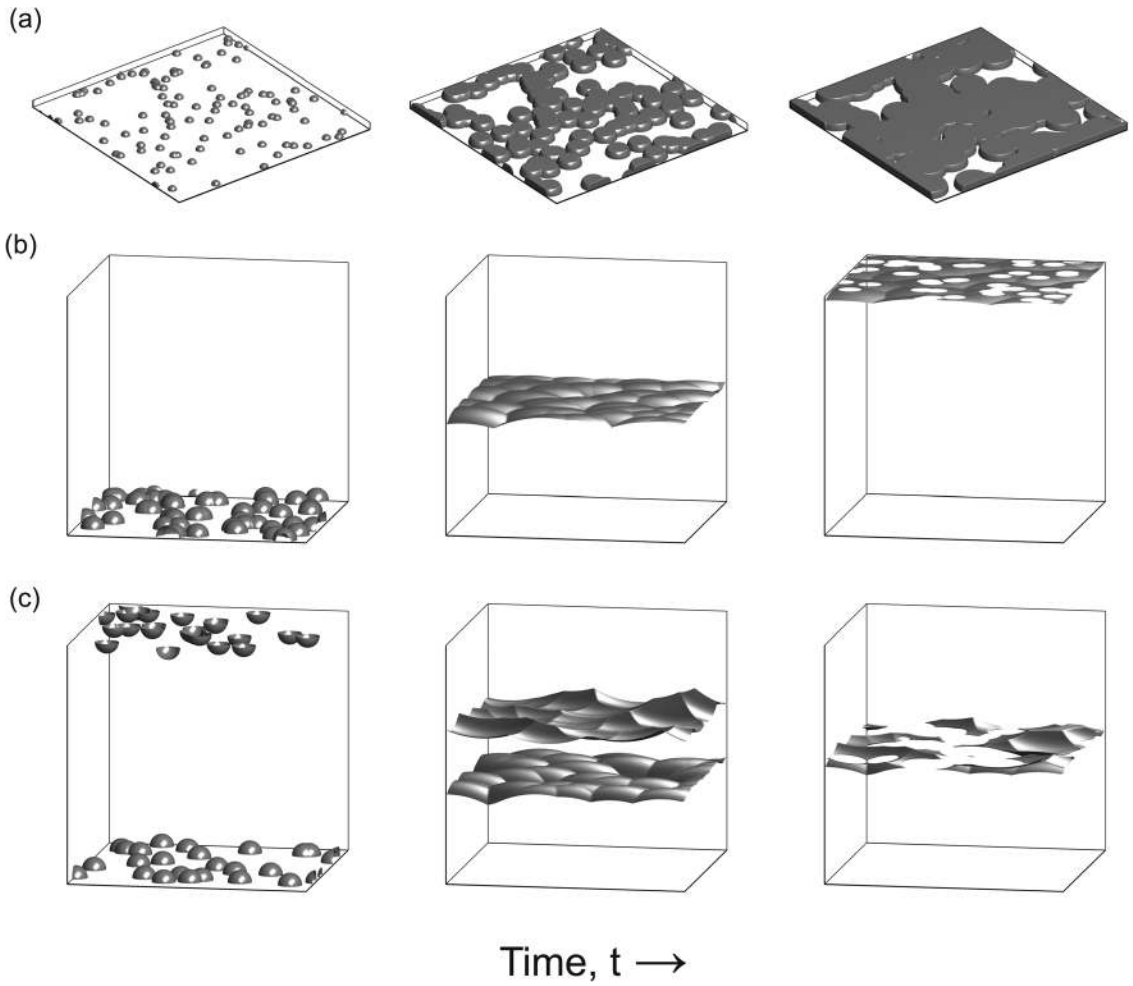

FIG. 6. Time evolution of the phase transformation process for the surface nucleation case. (a) 1-surface case, $h^* = 0.3$ (full view, $1500 \times 1500 \times 50$). (b) 1-surface case, $h^* = 7.3$ (section view, $50 \times 50 \times 50$). Only the interface is shown. (c) 2-surface case, $h^* = 5.2$ (section view, $50 \times 50 \times 50$). Only the interface is shown.

compared to the present work and also employed a nucleation density gradient through the film thickness, whereas in this work, we only studied the limiting cases of nuclei originating from one or two surfaces. Our results suggest that surface nucleation may in fact lead to increased values of the Avrami exponent at certain times during the transformation. In addition, our results suggest that finite-size effects do not necessarily lead to reduced values of the Avrami exponent as in the bulk nucleation case.

D. Discussion

As previously stated, a volume-fraction independent Avrami exponent assumes the validity of the JMAK equation. It has been demonstrated that, however, the assumptions of the JMAK equation can be grossly violated in thin film systems, and Eq. (4) is not valid in such cases. However, no simple and broadly applicable theory has superseded the JMAK theory in thin film systems, necessitating data analysis to be conducted using traditional methods by creating an Avrami plot and computing the Avrami exponent. We have applied this approach, even though we acknowledge its inapplicability in such situations, to analyze our simulation data in order to allow comparison to experiment.

The Avrami exponent has been shown to be non-constant throughout the phase transformation process in thin films, resulting in non-linear Avrami plots. Some authors have analyzed thin films by fitting a line to the entire Avrami plot to obtain a single averaged experimental value of n.[1,5] In light of the apparent non-linearity, we instead recommend analyzing the evolution of the local Avrami exponent, calculated by Eq. (8), over the course of the transformation.

Even the local Avrami exponent, however, does not necessarily correspond to the dimensionality of the transformation. Our results support the findings of other authors who assert that the Avrami exponent does not necessarily constitute concrete evidence of the dimensionality of phase transformations.[14,19] For the bulk nucleation case, n appears to correspond to the dimensionality of the transformation until the infinite size assumption begins to break down at high f_V; however, for the surface nucleation case, n rarely corresponds to the true dimensionality of the transformation. Thus, as more assumptions of the JMAK equation are violated, interpretation of the Avrami exponent becomes more difficult.

Analyzing behavior of the Avrami exponent over the entire transformation, however, can provide some evidence of the transformation mechanism. The flexibility of the

level-set model used in the present work allows simulation results to be fitted to experimental data. From this, transformation mechanisms and nucleation parameters of the real system can be inferred. While this method of fitting n vs. f_V over the entire transformation is more robust than fitting a single value of n, caution should still be used. Additional experimental evidence of microstructure, such as optical micrographs or TEM images, is preferred before drawing conclusions about transformation mechanisms.[3,4]

IV. CONCLUSIONS

The level-set method has been shown to be a simple yet versatile approach to study interface-controlled phase transformations, free of the assumptions behind the classical JMAK equation, and can be easily adapted to study a wide variety of problems. Only site-saturated nucleation with isotropic interface-kinetics controlled growth in thin films was considered in this paper. Effects of different parameters, including nucleation density, film thickness, and nucleation mode (bulk and surface), on the Avrami exponent and its evolution were determined.

By scaling lengths by a characteristic length of the system, which is a function of the nucleation density, the effects of film thickness and nucleation density are found to be dependent and can be encompassed in one parameter, the dimensionless film thickness h^*. h^* controls the evolution of the observed Avrami exponent.

The behavior of the Avrami exponent greatly differs between the bulk and surface nucleation cases. For the bulk nucleation case, finite-thickness effects lead to reduced Avrami exponents as the system transitions from 3D ($n = 3$) to 2D ($n = 2$) kinetics. Moreover, smaller h^* (smaller thickness and/or lower nucleation density) results in a transition to 2D kinetics at lower volume fractions f_V. For the surface nucleation case, however, finite-thickness effects do not necessarily lead to reduced Avrami exponents. In this scenario, the system transitions from 3D ($n \geq 3$) to 1D ($n \geq 1$) and/or 2D ($n = 2$) kinetics. When h^* is small (thin film and/or low nucleation density), the system transitions from 3D to 2D kinetics, and the transition occurs at lower f_V for smaller values of h^*. When h^* is large (large thickness and/or high nucleation density), however, the system transition from 3D to 1D kinetics, and the transition occurs at lower f_V for larger values of h^*. For intermediate values of h^*, hybrid behavior is observed as the system transitions from 3D to 1D to 2D kinetics.

The Avrami exponent has been shown to be non-constant throughout the transformation process in thin film systems, and its observed value may not necessarily correspond with the dimensionality of the transformation. Studying the behavior of the Avrami exponent over the process of the transformation, however, may allow transformation mechanisms and nucleation parameters to be inferred. Nonetheless, given the complicated temporal evolution of the Avrami exponent, care should be taken before drawing conclusions on the mechanism responsible for the transformation solely from the values of the Avrami exponent.

ACKNOWLEDGMENTS

The support of the NSF-MRSEC at Northwestern, DMR–1121262, is gratefully appreciated. E.L.P. also acknowledges the financial support of a Northwestern MRSEC REU award.

[1]D. Z. Hu, X. M. Lu, J. S. Zhu, and F. Yan, J. Appl. Phys. **102**, 113507 (2007).
[2]G. Gurato, D. Gaidano, and R. Zannetti, Makromol. Chem. **179**, 231 (1978).
[3]G. Ghosh, M. Chandrasekaran, and L. Delaey, Acta Metall. Mater. **39**, 925 (1991).
[4]J. C. Holzer and K. F. Kelton, Acta Metall. Mater. **39**, 1833 (1991).
[5]M. Quaas, H. Wulff, H. Steffen, and R. Hippler, Mater. Sci. Forum **378**, 320 (2001).
[6]M. H. Wang, H. Lei, Y. Seki, S. Seki, Y. Sawada, Y. Hoshi, S. H. Wang, and L. X. Sun, J. Therm. Anal. Calorim. **111**, 1457 (2013).
[7]M. Avrami, J. Chem. Phys. **7**, 1103 (1939).
[8]M. Avrami, J. Chem. Phys. **8**, 212 (1940).
[9]M. Avrami, J. Chem. Phys. **9**, 177 (1941).
[10]A. N. Kolmogorov, Bull. Acad. Sci. USSR Math. Ser. **1**, 355 (1937).
[11]W. A. Johnson and R. F. Mehl, Trans. Am. Inst. Min. Metall. Eng. **135**, 416 (1939).
[12]A. K. Jena and M. C. Chaturvedi, *Phase Transformation in Materials* (Prentice Hall, Englewood Cliffs, 1992).
[13]M. Weinberg and R. Kapral, J. Chem. Phys. **91**, 7146 (1989).
[14]L. E. Levine, K. L. Narayan, and K. F. Kelton, J. Mater. Res. **12**, 124 (1997).
[15]M. T. Todinov, Acta Mater. **48**, 4217 (2000).
[16]V. I. Trofimov, I. V. Trofimov, and J. I. Kim, Nucl. Instrum. Methods Phys. Res., Sect. B **216**, 334 (2004).
[17]N. V. Alekseechkin, Condens. Matter Phys. **11**, 597 (2008).
[18]J. Ocenasek, P. Novak, and S. Agbo, J. Appl. Phys. **115**, 043505 (2014).
[19]J. M. Schultz, Macromolecules **29**, 3022 (1996).
[20]N. Billon, J. M. Escleine, and J. M. Haudin, Colloid Polym. Sci. **267**, 668 (1989).
[21]J. M. Escleine, B. Monasse, E. Wey, and J. M. Haudin, Colloid Polym. Sci. **262**, 366 (1984).
[22]S. B. Lee, J. M. Rickman, and K. Barmak, Acta Mater. **51**(20), 6415 (2003).
[23]J. M. Rickman, W. S. Tong, and K. Barmak, Acta Mater. **45**(3), 1153 (1997).
[24]K. Sekimoto, Physica A **135**(2–3), 328 (1986).
[25]M. C. Weinberg, J. Non-Cryst. Solids **134**, 116 (1991).
[26]M. C. Weinberg, J. Non-Cryst. Solids **142**, 126 (1992).
[27]N. X. Sun, X. D. Liu, and K. Lu, Scripta Mater. **34**, 1201 (1996).
[28]S. Osher and R. Fedkiw, *Level Set Methods and Dynamic Implicit Surfaces* (Springer, New York, 2003).
[29]J. A. Sethian, *Level Set Methods and Fast Marching Methods: Evolving Interfaces in Computational Geometry, Fluid Mechanics, Computer Vision, and Materials Science* (Cambridge University Press, Cambridge, 1999).
[30]A. Calka and A. P. Radlinski, Mater. Sci. Eng. **97**, 241 (1988).